Astron. Astrophys. 338, L21–L24 (1998)

ASTRONOMY AND ASTROPHYSICS

LETTER

Letter to the Editor

Detection of the "44 μm" band of water ice in absorption in combined ISO SWS-LWS spectra⋆

E. Dartois[1], P. Cox[1], P.R. Roelfsema[2], A.P. Jones[1], A.G.G.M. Tielens[2], L. d'Hendecourt[1], M. Jourdain de Muizon[3], B. Schmitt[4], T. Lim[5], B. Swinyard[6], and A. M. Heras[5]

[1] Institut d'Astrophysique Spatiale, Bât. 121, Université Paris XI, F-91405 Orsay Cedex, France
[2] SRON, P.O. Box 800, 9700 AV Groningen, The Netherlands
[3] LAEFF, E-28080 Madrid, Spain & DESPA, Observatoire de Paris, F-92190 Meudon, France
[4] Laboratoire de Glaciologie et Géophysique de l'Environnement, CNRS, B.P. 96, F-38402 Grenoble/Saint-Martin d'Hères, France
[5] ISO Science Operations Centre, Astrophysics Division of ESA, P.O. Box 50727, E-28080 Madrid, Spain
[6] Rutherford Appleton Laboratory, Chilton, Didcot, Oxon OX11 0QX, UK

Received 20 July 1998 / Accepted 12 August 1998

Abstract. We report the detection of the transverse optical vibrational band of water ice at 44 μm in absorption towards two embedded infrared sources, IRAS 18316–0602 (RAFGL7009S) and IRAS 19110+1045. The water band extending from 30 to about 80 μm is a prominent feature in the combined ISO SWS and LWS grating spectra. Using new optical constants for amorphous and crystalline water ice, we have modeled the infrared spectra of the two embedded sources with a radiative transfer code. Most of the observed absorption bands are well fit by H_2O, CO, and CO_2 ice mantles on silicate and graphite cores.

Key words: ISM: dust, extinction – ISM: individual objects – infrared: ISM: continuum – infrared: ISM: lines and bands

1. Introduction

The wide spectral coverage provided by the combination of the Short Wavelength Spectrometer (SWS) and the Long Wavelength Spectrometer (LWS) on board the Infrared Space Observatory (ISO) enables for the first time a full view of both the continuum and the gas/dust signatures in a wide range of sources from 2.5 to 196.5 μm.

Absorption spectra of objects embedded in dense molecular clouds have established the dominant role of H_2O ice in molecular clouds. Water ice has strong bands throughout the infrared range with structures and positions which depend on its amorphous or crystalline state, e.g., Bertie et al. (1969) and Trotta & Schmitt (1998). H_2O ice was detected through the 3 μm stretching mode seen in absorption towards embedded infrared sources (Knacke et al. 1969, Gillett & Forrest 1973). Other bands were detected later: the bending mode at 6 μm by Russell et al. (1977), and the libration mode at 11 to 13.4 μm by Gillett & Soifer (1976) and Cox (1989). At longer wavelengths, the band of water ice near 40 μm has been reported in BN/KL in emission (Papoular et al. 1978) and absorption (Erickson et al. 1981), a difference attributed to the different beams sizes and the presence of radiative transfer effects. The 44 μm band of crystalline H_2O ice was later detected in emission by Omont et al. (1990) towards evolved oxygen-rich stars.

In this letter, we present combined ISO SWS and LWS spectroscopy of two embedded infrared sources, IRAS 18316–0602 (G25.7+1.1, RAFGL7009S) and IRAS 19110+1045 (G45.07+0.13). Both spectra display a series of strong absorption features including the water ice band at 44 μm. The massive protostar IRAS 18316–0602 has been mapped in the millimeter and submillimeter by McCutcheon et al. (1995) and was studied in detail by d'Hendecourt et al. (1996) and Dartois et al. (1998) who reported its exceptionally rich SWS absorption spectrum. For an adopted distance of 3.0 kpc, the infrared luminosity of IRAS 18316–0602 is $10^{4.3}$ $L_\odot$ (McCutcheon et al. 1995) which corresponds to a B0 ionizing star. IRAS 19110+1045 is a young protostar which has been investigated by Hunter et al. (1997). It is a compact, dense submillimeter source with evidence of infalling gas. It is associated with a high-velocity outflow and contains OH and H_2O masers (Hofner & Churchwell 1996). At an estimated distance of 8.3 kpc (Kuchar & Bania 1994), the infrared luminosity is $10^{5.8}$ $L_\odot$ and the spectral type of the ionizing star is O5.5.

2. Observations and results

The spectra of IRAS 18316–0602 and IRAS 19110+1045 were obtained during revolutions 152 (SWS only on IRAS 18316–0602), 478 and 499 (both sources, LWS and SWS). The 2.5–45 μm SWS grating spectra were taken in the full scan AOT1 mode (de Graauw et al. 1996) at speed 2 in rev. 478 and 499

Send offprint requests to: E. Dartois (e-mail: dartois@ias.fr)

⋆ Based on observations with ISO, an ESA project with instruments funded by ESA Member States (especially the PI countries: France, Germany, the Netherlands and the United Kingdom) and with the participation of ISAS and NASA

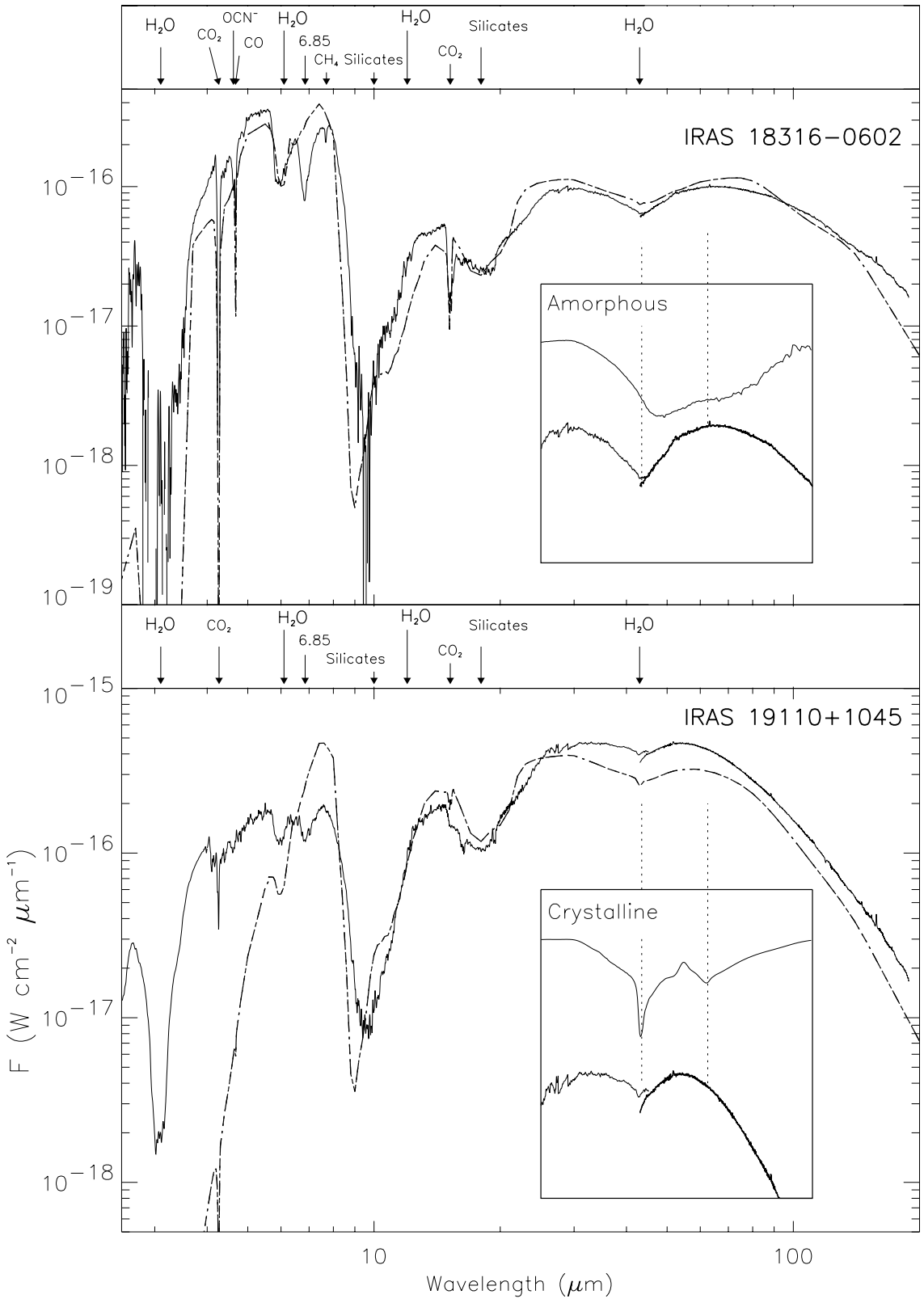

Fig. 1. Combined ISO SWS and LWS spectra of the embedded infrared sources IRAS18316–0602 (RAFGL7009S) and IRAS 19110+1045. The SWS and LWS spectra were calibrated independently and no corrections were made to improve the match between the two instruments. The positions and identifications of the main absorption bands are given for each source. The insert boxes display the transmittances of amorphous and crystalline water ices (from Trotta and Schmitt 1998) above the respective source spectra expanded for clarity. The results of radiative transfer calculations are shown as dash-dotted lines – see text for details.

and, at speed 3, in rev. 152. For IRAS 18316–0602, we combined both SWS data sets to improve the signal-to-noise. The data were processed using standard SWS Interactive Analysis procedures (de Graauw et al. 1996). Version 7.0 of the SWS off line processing (OLP) system flux and wavelength calibration was applied for the 12 AOT bands independently (Schaeidt et al. 1996; Valentijn et al. 1996). The final SWS spectra have a resolution of $\frac{\lambda}{\Delta\lambda} \sim 400$ and a wavelength accuracy better than one tenth of a resolution element. The absolute fluxes have an estimated accuracy of about 7% at the shortest wavelength to about 15% at 43 μm, with a significantly better relative spectral accuracy. The good agreement between the different independently calibrated AOT bands (see Fig. 1) indicates that the sources are true point sources for the SWS instrument. Residual calibration errors are present only in the 27–30 μm range (SWS AOT band 3E). In this wavelength range the relative spectral responsivity is not yet fully calibrated. Furthermore the good band to band agreement suggests that the error estimates are very conservative. The 43–196.5 μm LWS spectra were measured using the LWS AOT01 (Clegg et al. 1996). Each observation consisted of six fast grating scans with 0.5 sec integration ramps at each commanded grating position. The spectra were taken with four samples per resolution element. The absolute and relative flux calibration of the spectra is relative to Uranus (Swinyard et al. 1996). The data were reduced using the LWS off-line processing software (version 7.0). The ten sub-spectra, one for each detector, were then rescaled (with scaling factors not exceeding 15%) to the SW4 detector, considered to be one of the most photometrically reliable detectors.

The composite SWS and LWS spectra are shown in Fig. 1. No corrections were applied to match the SWS and LWS portions. The good agreement in the overlap region (41–43 μm) confirms the high quality of the flux scale calibration for the two instruments[1]. Both spectra are dominated by a series of bands which are identified in Fig. 1 – see, e.g., Whittet et al. (1996) and d'Hendecourt et al. (1996) for a description of the bands $\lesssim 25\mu$m. Centred on the overlap region between the SWS and LWS a broad absorption band is seen. With the accuracy of the calibration of the two spectrometers this cannot be explained as an instrumental feature. Furthermore, note that there are many SWS-LWS spectra of point sources with comparable fluxes at $\sim$ 40 μm which have continuous flat spectra without evidence of a broad absorption band at $\sim$ 43 μm (e.g., Roelfsema et al. 1998). Given the wavelength of the deepest absorption of 43 μm, we identify this band with the transverse optical (TO) vibrational band of water ice which is detected for the first time in absorption. In addition, in the region 20–30 μm, there is a shoulder on the 18 μm silicate feature which could be due to a refractory grain material.

[1] We wish to acknowledge the work of the SWS and LWS Instrument dedicated teams in VILSPA for the establishment and monitoring of the calibration. The SWS data were analysed using the SWS Interactive Analysis system developed and maintained jointly by SWS consortium members (Space Research Organisation of the Netherlands, Max Planck Institut für Extraterrestrische Physik, Katholieke Universiteit Leuven, European Space Agency).

The water ice band in IRAS 18316–0602 is strong and shows no substructure; this is consistent with absorption dominated by amorphous ice. In IRAS 19110+1045, the band is weaker and shows a small dip at $\sim 43\mu$m which indicates that the relative abundance of cristalline ice is higher in this source. However, comparison with the transmittance due to crystalline and amorphous ices (inserts in Fig. 1) indicates that the observed 44 μm band is different from the pure absorption case and that the band at 62 μm is not seen. We attribute these differences to temperature and opacity effects which become critical at wavelengths $\gtrsim$ 30 μm. Grains heated to 70 K have their peak emission at $\sim$ 44 μm and at this temperature water ice is stable against evaporation and can thus both emit and absorb. Hence radiation transfer can modify the structure of the far infrared H_2O ice band which is a combination of emission in the inner warmer regions and absorption in the outer colder regions. In addition, the high column densities in protostellar environments lead to significant extinction even at far-infrared wavelengths. This will alter the shape of the broad optical vibrational mode of H_2O ice which extends from 30 to 100 μm since the differential extinction $\tau_{30\mu m}/\tau_{100\mu m} \approx 5$. A transfer model is thus needed to determine the continuum level and to reproduce the details of the 44 μm band.

3. Model

We have written a simple radiative transfer model assuming a spherical geometry with a density power law as a free parameter. The best fits were found for $\mathrm{n(r)} \propto \mathrm{r}^{-1.4}$ for both sources, consistent with the distribution derived by Hunter et al. (1997) for IRAS 19110+1045. The central protostar is surrounded by a small, dust free, inner cavity defined by the evaporation temperature of the most refractory material, i.e. silicate at $\sim$ 1200 K. The outer radius defines the outer boundary of the region. The model calculates the radiative equilibrium temperature for a grain population of refractory cores made of silicates (pyroxenes, typical of protostars – Dorschner et al. 1995) and graphite (Draine & Lee 1984) with ice mantles. The effects of scattering were not taken into account because they are of lesser importance in the mid and far infrared. The ices consist of amorphous and crystalline water ices, together with CO_2 and CO ices as long as the grain temperature is below their respective sublimation temperatures. The temperature dependence of the ice properties has been taken into account. For the optical constants of the ices, we used the measurements by Trotta and Schmitt (1998). In the model, the H_2O ice is crystalline for $\mathrm{T} > 70$ K, amorphous at lower temperatures and evaporates above 100 K (Léger et al. 1983). The ices of CO_2 and CO evaporate above 70 K and 20 K, respectively. The bands at 6.8 μm, at 4.62 μm (attributed to OCN^- by Grim & Greenberg 1987) and the CH_4 band were not included.

4. Discussion and conclusions

The results of the transfer model are displayed in Fig. 1. Most of the absorption bands are reproduced in shape and width. In particular, the width and absorption depth of the 44 μm H_2O ice

band are well explained in both sources. The 62 μm band does not appear in the model spectra, consistent with the observed spectrum. The predicted strength of the 44 μm band is compatible with the strengths of the water ice bands at shorter wavelengths. In addition, the model reproduces the observed forms of the band: structureless in the case of IRAS 18316–0602 and with the additional dip at 43 μm in IRAS 19110+1045. These facts support the identification of the 43 μm band with the TO vibrational band of H_2O ice. However, for some of the bands the predicted shapes are different from those observed. In particular, the shape of the 3.0 μm band is not matched in detail because we have neglected scattering which begins to dominate when the grains are no longer small compared to the wavelength.

The estimated column densities of H_2O ice in IRAS 18316–0602 and IRAS 19110+1045 are $\sim 1.2 \times 10^{19}$ and $\sim 5 - -6 \times 10^{18}\,\mathrm{cm}^{-2}$, respectively. The relative abundances of the other ice constituents are $H_2O : CO_2 : CO$ (1:0.2:0.15) for IRAS 18316–0602 (see d'Hendecourt et al. 1996) and (1:0.05:<0.015) for IRAS 19110+1045. These numbers underscore the differences in the degree of evolution between the sources. IRAS 19110+1045 appears to be a more evolved protostar where significant ice mantle evaporation has already occured, consistent with the absence of CO and CH_4 ices, the weakness of the CO_2 band and the structure seen in the 43 μm band.

The visual extinction for the two protostars is also different. Adopting $\tau_{9.7\mu\mathrm{m}}/\mathrm{A_V} = 0.054\,\mathrm{mag}^{-1}$, we estimate $\mathrm{A_V} \gtrsim 40\,\mathrm{mag}$ and $\mathrm{A_V} \sim 25\,\mathrm{mag}$ for IRAS 18316–0602 and IRAS 19110+1045, respectively. We note that besides the apparent smaller silicate absorption the continuum of IRAS 19110+1045 shortward of 30 μm declines two orders of magnitude faster than the spectral energy distribution of IRAS 18316–0602, apparently in contradiction with the higher extinction found in the latter source. The poorer match of the model for the second source might be indicative of scattering effects in a non-spherical geometry arising from a strong bipolar outflow (as seen by Hunter et al. 1997), line of sight effects, e.g. a disk seen edge on, or additional absorption not taken into account in the model. The presence of crystalline H_2O ice in IRAS 19110+1045, as indicated by the water ice TO band structure is further strengthened by the shape of the 6 μm band even if these two modes partly originate from different regions. The presence of crystalline ice in some protostellar environments has been inferred from substructure observed in the 3 μm band (Smith et al. 1989). Further investigation of this band from the ground could constrain the crystallinity of the ice in this source.

In conclusion, it is important to note that the detection and the simulation of the broad 44 μm water ice transverse optical vibrational band would not have been possible without spectroscopy over the wide wavelength range provided by the combined SWS-LWS spectra. Other less abundant components of interstellar ices (e.g. NH_3, Lacy et al. 1998) may be very difficult to detect in the far-infrared. The long wavelength modes are lattice modes which will weaken or vanish as soon as the material is diluted in an other matrix. Nevertheless, the detection of some of these modes in ISO spectra of deeply embedded sources would provide important information on the structure of grain mantles in the interstellar medium.

References

Bertie, J.E., Labbé, H.J., Whalley, E. 1969, J. Chem. Phys. 50, 4501.
Clegg, P.E. et al. 1996, A&A 315, L38
Cox, P. 1989, A&A 225, L1
Dartois, E., et al. 1998, A&A 331, 651
Dorschner J. et al. 1995, A&A, 300, 503.
Draine, B.T., Lee, H.M. 1984, ApJ 285, 89
Erickson, E.F., et al. 1981, ApJ 245, 148.
Gillett, F.C., Forrest, W.J. 1973, ApJ 179, 483.
Gillett, F.C., Soifer, B.T. 1976, ApJ, 207, 780
Grim, R.J.A., Greenberg, J.M. 1987, A&A, 181, 155.
de Graauw, T. et al. 1996, A&A, 315, L345
d'Hendecourt, L. et al. 1996, A&A 315, L365
Hofner, P., Churchwell, E. 1996, A&AS 120, 283
Hunter, T.R., Phillips, T.G., Menten, K.M. 1997, ApJ 478, 283
Knacke, R.F., Cudabak, D.D., Gaustad, J.E. 1969, ApJ 158, 151
Kuchar, T.A., Bania, T.M. 1994, ApJ 436, 117
Lacy et al. 1998, ApJ 501, L105.
Léger et al. 1983, A&A 117, 164.
McCutcheon, W.H. et al. 1995 AJ 110, 1762
Omont, A. et al. 1990, ApJ 355, L27
Papoular, R. et al., 1978, Nature 276, 593
Roelfsema, P.R. et al., 1998, in ASP Conf. Ser. 132: Star Formation with the Infrared Space Observatory, p.76
Russell, R.W., Soifer, B.T., Puetter, R.C. 1977, A&A 54, 959.
Schaeidt S.G. et al. 1996, A&A 315, L55.
Smith, R.G., Sellgren, K., Tokunaga A.T. 1989, ApJ 344, 413.
Swinyard, B. et al. 1996, A&A 315, L43
Trotta F., Schmitt B., 1998, Applied Spectroscopy, in prep.
Valentijn E.A. et al. 1996, A&A 315, L60.
Whittet D.C.B., et al. 1996, A&A 315, L357